

Crystal structures and property characterization of two magnetic frustration compounds

Kunkun Li,^{1,2} Duanduan Yuan,^{1,2} Shijie Shen,³ and Jiangang Guo^{1,a)}

¹Beijing National Laboratory for Condensed Matter Physics, Institute of Physics, Chinese Academy of Sciences, Beijing 100190, China

²University of Chinese Academy of Sciences, Beijing 100049, China

³Department of Physics & Electronic Engineering, Taizhou University, Taizhou 318000, China

(Received 2 April 2018; accepted 13 May 2018)

We report the structure and physical properties of two quasi-two-dimensional triangular antiferromagnetic materials, $\text{Co}_{0.66}\text{Al}_2\text{Se}_{3.53}$ and $\text{Ni}_{0.61}\text{Al}_2\text{Se}_{3.55}$, which show highly magnetically frustrated characters. Powder X-ray diffractions demonstrate that $\text{Co}_{0.66}\text{Al}_2\text{Se}_{3.53}$ and $\text{Ni}_{0.61}\text{Al}_2\text{Se}_{3.55}$ possess identical space group of $P-3m1$ with lattice parameters $a = 3.8089(1) \text{ \AA}$, $c = 12.676(1) \text{ \AA}$ and $a = 3.7880(1) \text{ \AA}$, $c = 12.650(1) \text{ \AA}$, respectively. Analyzing the susceptibility data of $\text{Co}_{0.66}\text{Al}_2\text{Se}_{3.53}$ reveal a Curie Weiss temperature of -216 K , and a spin-freezing transition temperature of 4.5 K , giving a frustration index $f = -\theta_{\text{CW}}/T_{\text{f}} \approx 48$. $\text{Ni}_{0.61}\text{Al}_2\text{Se}_{3.55}$ possesses an effective moment of $2.38 \mu_{\text{B}}$, a Curie–Weiss temperature of -62 K with no sign of spin-freezing transition down to 2 K . The AC susceptibility data of $\text{Co}_{0.66}\text{Al}_2\text{Se}_{3.53}$ suggest a spin glass-like transition, but no intersite mixing between Co^{2+} and Al^{3+} was observed from the X-ray photoelectron spectroscopy measurements. © 2018 International Centre for Diffraction Data. [doi:10.1017/S0885715618000507]

Key words: geometrical frustration, triangular lattice, powder diffraction, Rietveld refinement, spin freezing

I. INTRODUCTION

The discovery of superconductivity in alkali iron selenides has sparked widespread renewal interest in searching new superconductors in this class of layered compounds (Guo *et al.*, 2010). Lots of novel compounds have been synthesized and characterized, including the co-intercalated superconductors $\text{A}_x(\text{NH}_3)_y\text{Fe}_2\text{Se}_2$ ($A = \text{Li}, \text{Na}, \text{Ba}, \text{Sr}, \text{Ca}, \text{Yb}, \text{and Eu}$) (Ying *et al.*, 2012, 2013), $\text{Na}_x(\text{En})_y\text{Fe}_2\text{Se}_2$ (Jin *et al.*, 2017), and $(\text{Li}_{0.8}\text{Fe}_{0.2})\text{OHFeSe}$ (Lu *et al.*, 2014); Cs vacancy ordered material $\text{CsFe}_{4-\delta}\text{Se}_4$ without phase separation (Li *et al.*, 2018); rhombohedral and hexagonal materials $\text{Li}_x\text{Fe}_7\text{Se}_8$ (Ying *et al.*, 2016), $\text{NaFe}_{1.6}\text{S}_2$ (Lai *et al.*, 2013), and CaOFeS (Jin *et al.*, 2015); and other transition metal-based materials KMnAgSe_2 (Lai *et al.*, 2014) and $\text{Ba}_2\text{MO}_2\text{Ag}_2\text{Se}_2$ ($M = \text{Co}, \text{Mn}$) (Zhou *et al.*, 2014) as well. Similar to the case of cuprates (Chen *et al.*, 1992, 1995a, c; Tu *et al.*, 2001), iron-based superconductors have a close relation with the suppression of magnetic long-range ordering by carrier doping, orbital hybridization, external pressures, and chemical pressures. Geometrical frustration, a phenomenon arising from the competing magnetic interactions that cannot all favor a same ordered state because of local geometric constraints, exhibits no magnetic long-range ordering. It is expected to play a role in inducing superconductivity by suppressing antiferromagnetism and might have a connection with new unconventional superconductors (Anderson, 1987; Collins and Petrenko, 1997).

As the simplest form of a geometrically frustrated lattice in two dimensions, the triangular lattice with an antiferromagnetic coupling single magnetic atom per unit cell has been extensively studied for searching spin-disordered states ever since a quantum spin-disordered state was first proposed by Anderson (Anderson, 1973). Up to now, only a few triangular lattice antiferromagnets have been reported to be a spin-disordered state, such as the organic materials κ -(BEDT-TTF)₂Cu₂(CN)₃ (Shimizu *et al.*, 2003), $\text{EtMe}_3\text{Sb}[\text{Pd}(\text{mit})_2]_2$ (Itou *et al.*, 2008), and inorganic materials NiGa_2S_4 (Nakatsuji *et al.*, 2005), FeGa_2S_4 (Nakatsuji *et al.*, 2007), and FeAl_2Se_4 (Li *et al.*, submitted). NiGa_2S_4 is the first example of a low-spin ($S = 1$) antiferromagnet with one Ni atom site on each triangular lattice point. Two triangular lattice antiferromagnets $\text{Na}_x\text{CoO}_2 \cdot y\text{H}_2\text{O}$ (Takada *et al.*, 2003) and κ -(BEDT-TTF)₂Cu₂(CN)₃ (Kurosaki *et al.*, 2005) have been reported to possess superconductivity through doping or pressure.

Here we report the synthesis and characterization of two quasi-two-dimensional (2D) triangular antiferromagnetic materials $\text{Co}_{0.66}\text{Al}_2\text{Se}_{3.53}$ and $\text{Ni}_{0.61}\text{Al}_2\text{Se}_{3.55}$ with $S = 3/2$ and 1, respectively. Our results suggest that $\text{Co}_{0.66}\text{Al}_2\text{Se}_{3.53}$ and $\text{Ni}_{0.61}\text{Al}_2\text{Se}_{3.55}$ are highly frustrated magnetic materials that are isostructural with FeAl_2Se_4 . $\text{Co}_{0.66}\text{Al}_2\text{Se}_{3.53}$ possesses an effective moment of $4.92 \mu_{\text{B}}$ with a high frustration index of 48. AC susceptibility and X-ray photoelectron spectroscopy (XPS) measurements suggest a spin glass-like transition, which is not induced by intersite mixing disorder. On the other hand, $\text{Ni}_{0.61}\text{Al}_2\text{Se}_{3.55}$ possesses an effective moment of $2.38 \mu_{\text{B}}$, a Curie–Weiss temperature of -62 K with no sign of spin-freezing transition down to 2 K . The stronger magnetic frustration in the case of $\text{Co}_{0.66}\text{Al}_2\text{Se}_{3.53}$ and

^{a)} Author to whom correspondence should be addressed. Electronic mail: jgguo@iphy.ac.cn

$\text{Ni}_{0.61}\text{Al}_2\text{Se}_{3.55}$ should originate from the relatively small spin of 3/2 and 1 for $\text{Co}_{0.66}\text{Al}_2\text{Se}_{3.53}$ and $\text{Ni}_{0.61}\text{Al}_2\text{Se}_{3.55}$, respectively.

II. EXPERIMENTAL

Polycrystalline samples of $\text{Co}_{0.7}\text{Al}_2\text{Se}_{3.7}$ and $\text{NiAl}_2\text{Se}_{3.7}$ were prepared via conventional solid-state method using Co powder, Ni powder, Al wire, and Se shot (Alfa, 99.999, 99.999, 99.9, and 99.999%, respectively) as starting materials. Al_2Se_3 precursors were prepared via the reaction of Al wire and Se shot at 1150 K for 24 h in sealed quartz tubes. CoSe and NiSe precursors were prepared via the reaction of Co/Ni powder and Se powder at 1150 K for 24 h in sealed quartz tubes. The obtained Al_2Se_3 precursors together with stoichiometric amount of CoSe/NiSe precursors were pulverized, pressed into a pellet, sealed in a quartz tube with Ar gas, and then heated and kept at 1073 K for 72 h. The obtained polycrystalline samples were black and air-sensitive. Because of the sensitivity to air and moisture of raw materials, all operations were performed in an argon-filled glove box.

Room temperature powder X-ray diffraction (PXRD) data were collected using a PANalytical X'Pert PRO diffractometer ($\text{CuK}\alpha$ radiation) with a graphite monochromator in a reflection mode from $2\theta = 10^\circ$ to 130° and $\text{step} = 0.017^\circ$ (Chen *et al.*, 1995b). Rietveld refinements were performed with the FULLPROF package (Rodriguez-Carvajal, 2001). The magnetic susceptibilities were measured using a vibrating sample magnetometer (VSM, Quantum Design). AC magnetizations were measured on a Magnetic Properties Measurement System (MPMS, Quantum Design). The XPS measurements were performed with an ESCALAB Mk II (Vacuum Generators) spectrometer using $\text{AlK}\alpha$ X-rays (240 W). The binding energies were calibrated against the C 1s signal (284.8 eV) of adventitious carbon.

III. RESULTS AND DISCUSSION

Figure 1(a) and (b) show the PXRD patterns of polycrystalline $\text{Co}_{0.7}\text{Al}_2\text{Se}_{3.7}$ and $\text{NiAl}_2\text{Se}_{3.7}$ sample collected at room temperature, respectively. The reflection peaks could be indexed with a trigonal symmetry with lattice parameters $a = 3.8089(1) \text{ \AA}$, $c = 12.676(1) \text{ \AA}$ for $\text{Co}_{0.7}\text{Al}_2\text{Se}_{3.7}$ and $a = 3.7880(1) \text{ \AA}$, $c = 12.650(1) \text{ \AA}$ for $\text{NiAl}_2\text{Se}_{3.7}$, respectively. According to the extinction conditions, the possible space group is $P\bar{3}m1$ (No. 164), which is isostructural with the previously reported compound FeAl_2Se_4 . Adopting the possible space group $P\bar{3}m1$, the indexed values of $2\theta_{\text{obs}}$, $2\theta_{\text{cal}}$, $\Delta 2\theta$, d_{obs} , d_{cal} , I_{obs} , and (hkl) are listed in Supplementary materials with the figures of merit $F(30) = 68.7(0.007, 72)$ for $\text{Co}_{0.7}\text{Al}_2\text{Se}_{3.7}$ and $F(30) = 91.2(0.0041, 83)$ for $\text{NiAl}_2\text{Se}_{3.7}$, respectively. Compared with the reported lattice parameters $a = 3.8335(1) \text{ \AA}$, $c = 12.737(1) \text{ \AA}$ in FeAl_2Se_4 , the lattice parameter a of $\text{Co}_{0.7}\text{Al}_2\text{Se}_{3.7}$ and $\text{NiAl}_2\text{Se}_{3.7}$ shrinks by 0.64 and 1.19%, while c shrinks by 0.48 and 0.68%, respectively. The evolution of lattice parameters is reasonable, considering the gradual decrease of ionic radius for Fe^{2+} , Co^{2+} , and Ni^{2+} . Rietveld refinements against the PXRD data were performed by adopting the FeAl_2Se_4 structure as an initial model. Considering the volatility of Se and the reported isostructural compound $\text{Ni}_{0.7}\text{Al}_2\text{S}_{3.7}$, we set occupancy of Al atom to be 1 (Higo *et al.*, 2011). The refinements smoothly converged to $R_p = 4.22\%$, $R_{\text{wp}} = 6.19\%$, $R_{\text{exp}} = 2.41\%$ for $\text{Co}_{0.7}\text{Al}_2\text{Se}_{3.7}$ and $R_p = 2.99\%$, $R_{\text{wp}} = 4.36\%$, $R_{\text{exp}} = 2.67\%$ for $\text{NiAl}_2\text{Se}_{3.7}$, respectively. The sample compositions determined from the refinement are $\text{Co}_{0.66}\text{Al}_2\text{Se}_{3.53}$ and $\text{Ni}_{0.61}\text{Al}_2\text{Se}_{3.55}$, respectively, which are used in the text hereafter. We calculate the theoretical density of both samples, which are 3.86 and 3.91 g cm^{-3} for $\text{Co}_{0.66}\text{Al}_2\text{Se}_{3.53}$ and $\text{Ni}_{0.61}\text{Al}_2\text{Se}_{3.55}$, respectively. The composition of $\text{Co}_{0.7}\text{Al}_2\text{Se}_{3.7}$ was checked by inductively coupled plasma atomic emission spectrometer, giving an atomic ratio of $\text{Co}_{0.69}\text{Al}_2\text{Se}_{3.61}$, consistent with our Rietveld refinements. The reason for the large quantity

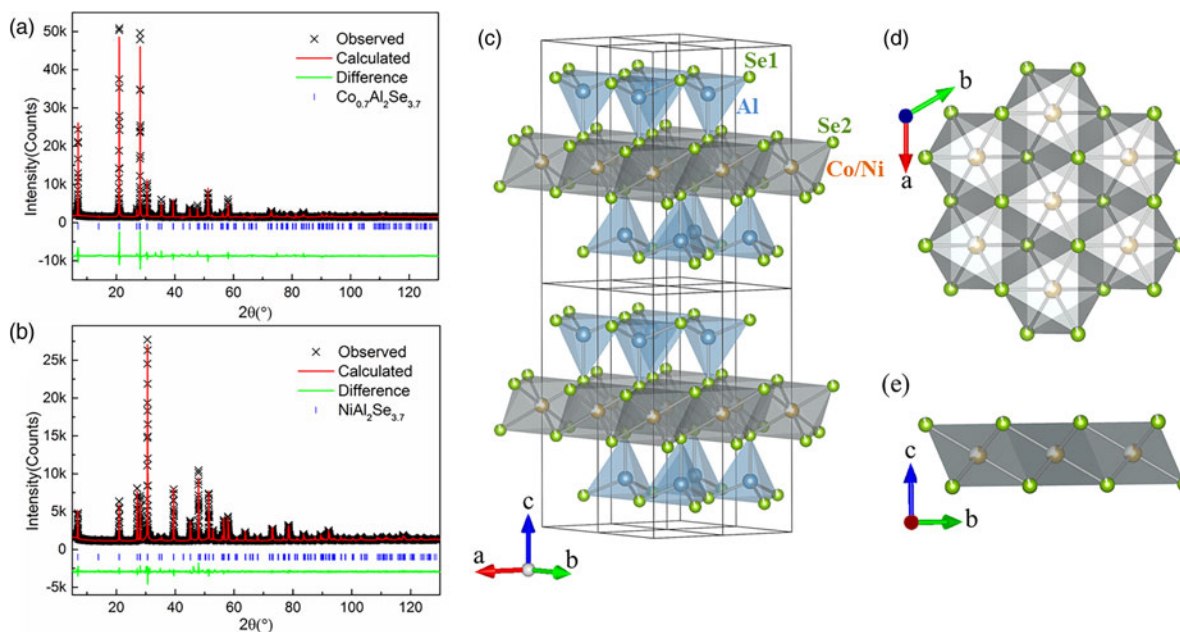


Figure 1. (Color online) (a)–(b) Powder X-ray diffractions and Rietveld refinements of $\text{Co}_{0.7}\text{Al}_2\text{Se}_{3.7}$ and $\text{NiAl}_2\text{Se}_{3.7}$ at room temperature, respectively. (c) The schematic crystal structure of $\text{Co}_{0.7}\text{Al}_2\text{Se}_{3.7}/\text{NiAl}_2\text{Se}_{3.7}$. (d) The crystal structure of $\text{CoSe}_6/\text{NiSe}_6$ octahedral layer viewed along [001] direction. (e) The crystal structure of $\text{CoSe}_6/\text{NiSe}_6$ octahedral layer viewed along [100] direction.

of vacancies in the proposed structure is not quite clear. But based on previous reports, NiGa_2S_4 is full occupancy while $\text{Ni}_{0.7}\text{Al}_2\text{S}_{3.7}$ possesses a large quantity of vacancies. Since atom radius is crucial for holding a structure, we can infer that the small atom radius of Al compared with Ga might be responsible for this phenomenon. Detailed structural parameters are listed in Table I. As shown in Figure 1(c), the compound is built by stacking of layers consisting of edge-sharing $\text{CoSe}_6/\text{NiSe}_6$ octahedra connected by a top and a bottom sheet of AlSe_4 tetrahedra. The layer spacing is separated with each other by a van der Waals gap. Figure 1(d) and (e) shows the central $\text{CoSe}_6/\text{NiSe}_6$ octahedra layer viewed along the [001] and [100] direction. The Co/Ni ions form a triangular lattice plane, which is isostructural to the CoO_2 layer of the known superconductor $\text{Na}_x\text{CoO}_2 \cdot y\text{H}_2\text{O}$. The $\text{CoSe}_6/\text{NiSe}_6$ octahedra probably gives Co^{2+} and Ni^{2+} a $t_{2g}^4 e_g^2$ configuration with a high spin $S = 3/2$ and 1, respectively (Nakatsuji *et al.*, 2007).

Figure 2(a) shows the temperature-dependent DC magnetic susceptibility χ and its inverse χ^{-1} under applied fields of 0.01, 1, and 8 T for $\text{Co}_{0.66}\text{Al}_2\text{Se}_{3.53}$. A bifurcation (denoted as T_f) at 4.5 K can be seen under 0.01 T for $\text{Co}_{0.66}\text{Al}_2\text{Se}_{3.53}$, which is suppressed when the applied field reaches 1 T. This transition is probably associated with a spin-freezing transition (Mydosh and Ebrary, 1993). The temperature-dependent susceptibility from 100 to 300 K obeys the Curie–Weiss law $\chi = C/(T - \theta_{\text{cw}})$, where C is the Curie constant and θ_{cw} the Weiss temperature as illustrated in the inset of Figure 2(a). An effective moment of $4.92 \mu_B$ was obtained from the fitted Curie constant. The Weiss temperature $\theta_{\text{cw}} = -216$ K indicates strong antiferromagnetic interactions. The frustration index, defined by $f = -\theta_{\text{cw}}/T_f$, is estimated as 48, which is a relatively large value compared with FeAl_2Se_4 (Li *et al.*, unpublished). Thus, we conclude that $\text{Co}_{0.66}\text{Al}_2\text{Se}_{3.53}$ is a highly magnetically frustrated system. Figure 2(b) shows the temperature-dependent DC magnetic susceptibility χ and its inverse χ^{-1} for $\text{Ni}_{0.61}\text{Al}_2\text{Se}_{3.55}$. Unlike FeAl_2Se_4 and $\text{Co}_{0.66}\text{Al}_2\text{Se}_{3.53}$, no

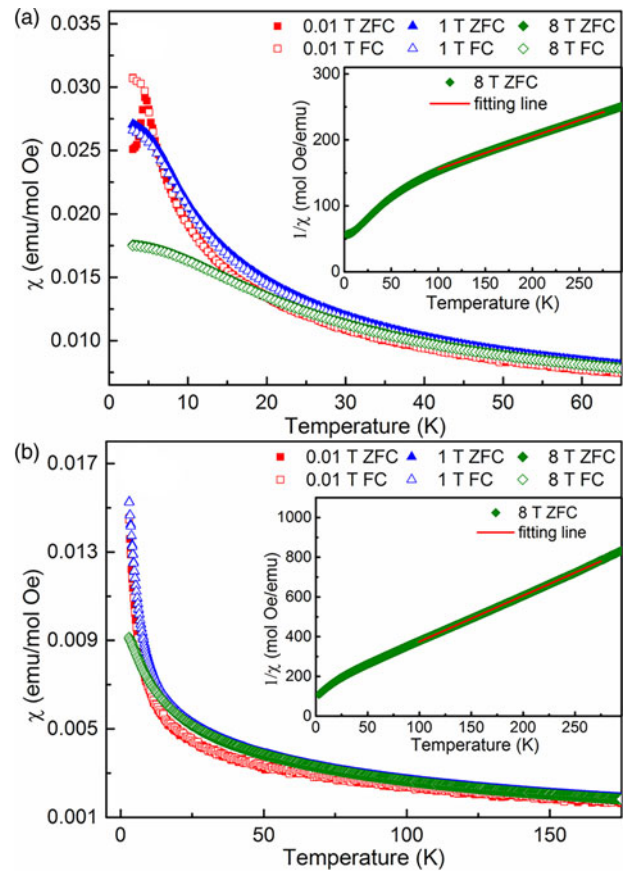


Figure 2. (Color online) (a)–(b) Zero-field-cooled (ZFC) and field-cooled (FC) χ (T) data taken under different applied fields from 2 to 300 K for $\text{Co}_{0.66}\text{Al}_2\text{Se}_{3.53}$ and $\text{Ni}_{0.61}\text{Al}_2\text{Se}_{3.55}$, respectively. Inset: the inverted $\chi^{-1}(T)$ data with an applied field of 8 T. The solid red lines are linear fits with a Curie–Weiss law $\chi = C/(T - \theta_{\text{cw}})$.

TABLE I. Room temperature structure details of $\text{Co}_{0.66}\text{Al}_2\text{Se}_{3.53}$ and $\text{Ni}_{0.61}\text{Al}_2\text{Se}_{3.55}$.

	$\text{Co}_{0.66}\text{Al}_2\text{Se}_{3.53}$	$\text{Ni}_{0.61}\text{Al}_2\text{Se}_{3.55}$
Space group	$P-3m1$ (164)	$P-3m1$ (164)
a (Å)	3.80891 (4)	3.78801 (3)
c (Å)	12.67626 (14)	12.65015 (11)
V (Å ³)	159.26 (1)	157.20 (1)
Atomic parameters		
Co/Ni ($1b$)	(0,0,1/2)	(0,0,1/2)
Occupation	0.657 (8)	0.609 (10)
B_{iso} (Å ²)	1.636 (233)	0.594 (191)
Al ($2d$)	[1/3,2/3,0.1947(2)]	[1/3,2/3,0.2043(4)]
Occupation	1	1
B_{iso} (Å ²)	1.286 (166)	2.020 (155)
Se1 ($2d$)	[1/3,2/3,0.3925(2)]	[1/3,2/3,0.3934(2)]
Occupation	0.860 (9)	0.874 (9)
B_{iso} (Å ²)	0.960 (85)	0.586 (58)
Se2 ($2d$)	[1/3,2/3,0.8658(2)]	[1/3,2/3,0.8664(3)]
Occupation	0.903 (12)	0.901 (12)
B_{iso} (Å ²)	1.108 (77)	1.137 (58)
Agreement factors		
R_p	3.52%	2.99%
R_{wp}	5.57%	4.36%
R_{exp}	2.41%	2.67%
χ^2	5.33	2.67

bifurcation down to 2 K can be seen under a field of 0.01 T. However, fitting the temperature-dependent susceptibility from 100 to 300 K with the Curie–Weiss law gives an effective moment of $2.38 \mu_B$ and Weiss temperature θ_{cw} of -62 K, indicating a strong magnetically frustrated system.

To characterize the magnetism of $\text{Co}_{0.66}\text{Al}_2\text{Se}_{3.53}$ at temperatures near the bifurcation, we measured its temperature-dependent AC susceptibility from 2 to 10 K at different frequencies. As shown in Figure 3, a peak at about 4.5 K is observed in the real part, which is the signature of the susceptibility bifurcation. A small but clear peak shift towards high temperatures can be seen as increasing frequency, which suggests a spin relaxation behavior. The shift of the peak temperature as a function of frequency described by the expression, $(\Delta T_f)/(T_f \Delta \log \omega)$, can be used to distinguish spin glass and spin glass-like materials (Mydosh and Ebrary, 1993; Krizan and Cava, 2014). The value obtained for $\text{Co}_{0.66}\text{Al}_2\text{Se}_{3.53}$ is 0.038, which is slightly larger than expected for a canonical spin glass but is in the range of spin glass-like materials. The Volger–Fulcher law is then applied to characterize the relaxation feature with a function correlating the bifurcation temperature (T_f) and frequency (f): $T_f = T_0 - (E_a)/(k_B) 1/\ln(\tau_0 f)$, where τ_0 is the intrinsic relaxation time, E_a the activation energy of the process, and T_0 the ideal glass temperature (Mydosh and Ebrary, 1993). Fixing the ideal glass temperature $T_0 = 4.5$ K, the obtained relaxation time τ_0 is 5.4×10^{-10} s, and the activation energy E_a is 0.14 meV. It should

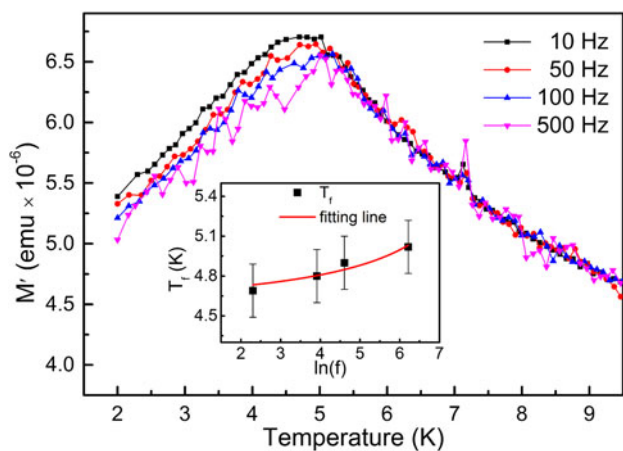


Figure 3. (Color online) Temperature dependence of the real part of the AC magnetic susceptibilities as a function of frequency for $\text{Co}_{0.66}\text{Al}_2\text{Se}_{3.53}$ sample. Inset shows the parameterization of the spin freezing (as determined by the AC susceptibility) and fitting line to the Vogel–Fulcher law.

be noted that the small peak at approximately 7 K originates from the instrument error.

Spin glass transition usually originates from atom disorder in the compounds; thus, XPS measurements were carried out to check the intersite mixing between Co^{2+} and Al^{3+} . Figure 4(a) shows Co 2*p* spectra of the $\text{Co}_{0.66}\text{Al}_2\text{Se}_{3.53}$ samples. Because of the spin–orbit coupling, the Co 2*p* spectra were split into two different parts: Co 2*p*_{3/2} and Co 2*p*_{1/2}, the fitted binding energy

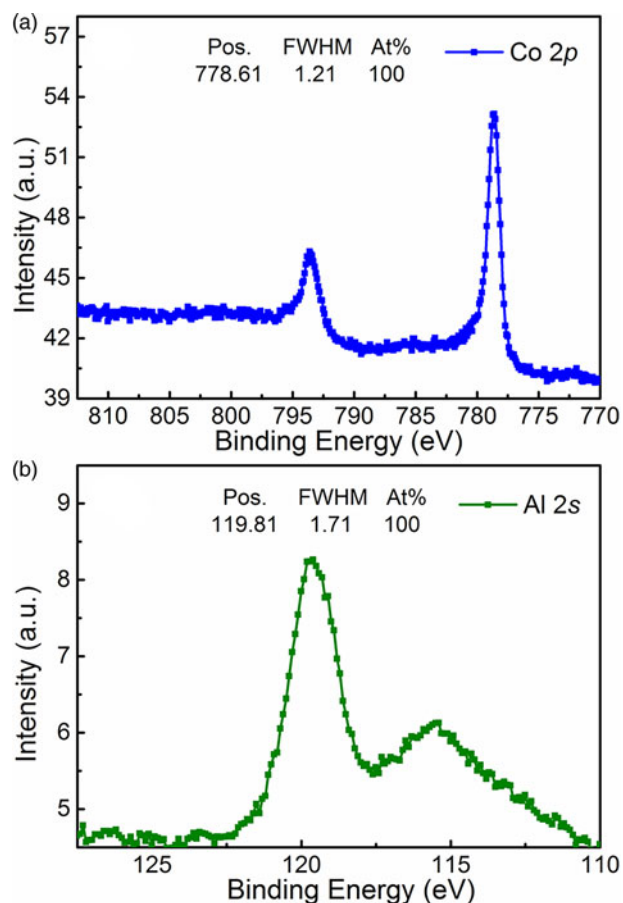


Figure 4. (Color online) XPS spectra of $\text{Co}_{0.66}\text{Al}_2\text{Se}_{3.53}$ sample for Co 2*p* (a) and Al 2*s* (b).

values are 793.6 and 778.6 eV. The full width at half maximum (FWHM) of the peak of Co 2*p*_{1/2} is 1.21. Figure 4(b) shows Al 2*s* spectra of the $\text{Co}_{0.66}\text{Al}_2\text{Se}_{3.53}$ samples. The fitted binding energy value is 119.8 eV with FWHM of 1.71, corresponding to that of the previously reported Co^{2+} and Al^{3+} oxidation states (McGuire *et al.*, 1973; Mandale *et al.*, 1984). No sign of widening and unsymmetrical can be observed from the peak shape, indicating there is no sign of intersite mixing between Co^{2+} and Al^{3+} (Zha *et al.*, 2016). Thus, the observed spin glass transition should not originate from the intersite mixing disorder between Co^{2+} and Al^{3+} ions.

The reported isostructural FeAl_2Se_4 compound possesses a spin-freezing transition at $T_f = 14$ K with a frustration index of 14. For $\text{Co}_{0.66}\text{Al}_2\text{Se}_{3.53}$ samples, although there is no intersite mixing between Co^{2+} and Al^{3+} , susceptibility measurements yield a spin-freezing transition at $T_f = 4.5$ K with a frustration index of 48, nearly three times larger than that in FeAl_2Se_4 compound. In the case of $\text{Ni}_{0.61}\text{Al}_2\text{Se}_{3.55}$ samples, no sign of spin-freezing transition can be observed down to 2 K with a Weiss temperature θ_{cw} of -62 K. As Collins and Petrenko showed, magnetic frustration would occur in a 2D triangular lattice, if no disturbance occurs from other sources such as interlayer coupling or magnetic impurities (Collins and Petrenko, 1997). In our case, the stoichiometric FeAl_2Se_4 shows spin-freezing transition, while $\text{Ni}_{0.61}\text{Al}_2\text{Se}_{3.55}$ shows no sign of spin-freezing transition with vacancies. Thus, we can speculate that vacancies might not be crucial for magnetic properties and its impact on these three materials needs further investigation. Moreover, the fluctuations of the spins in a spin liquid can be classical or quantum. For systems with large *S*, classical spin fluctuations dominate and are driven by thermal activation energy. Spins can be thought of as reorienting randomly with time, cycling through different microstates. When the energy $k_B T$ becomes too small, classical fluctuations cease and the spins either freeze or order (Balents, 2010). With *S* being comparable to 1/2, energy change because of the spin flips is relatively small. Entangled spin pairs will remain to have a considerable lifetime. The fluctuations because of the spin flips will result in a large number of states with the same energy, i.e. the quantum spin liquid, which can persist down to $T = 0$ K. Thus, a transition from spin liquid to spin glass is possible when the spin changes from $S = 1/2$ in $\text{Lu}_2\text{Mo}_2\text{O}_5\text{N}_2$ to $S = 1$ $\text{Lu}_2\text{Mo}_2\text{O}_7$ (Clark *et al.*, 2014). Therefore, it can be understood that the magnetic frustration becomes stronger from the case of FeAl_2Se_4 to $\text{Co}_{0.66}\text{Al}_2\text{Se}_{3.53}$ and $\text{Ni}_{0.61}\text{Al}_2\text{Se}_{3.55}$.

IV. CONCLUSION

In conclusion, we discover two quasi-2D triangular anti-ferromagnetic materials $\text{Co}_{0.66}\text{Al}_2\text{Se}_{3.53}$ and $\text{Ni}_{0.61}\text{Al}_2\text{Se}_{3.55}$ for the first time. Our results suggest that $\text{Co}_{0.66}\text{Al}_2\text{Se}_{3.53}$ and $\text{Ni}_{0.61}\text{Al}_2\text{Se}_{3.55}$ are highly frustrated magnetic materials. The susceptibility data analyses reveal an effective moment for the Co^{2+} of $4.92 \mu_B$, a high Curie–Weiss temperature of -216 K and a spin-freezing transition of 4.5 K in $\text{Co}_{0.66}\text{Al}_2\text{Se}_{3.53}$, which gives a frustration index $f = -\theta_{\text{cw}}/T_f \approx 48$. $\text{Ni}_{0.61}\text{Al}_2\text{Se}_{3.55}$ possesses an effective moment of $2.38 \mu_B$ and a Curie–Weiss temperature of -62 K, with no sign of spin-freezing transition down to 2 K. The AC susceptibility data of $\text{Co}_{0.66}\text{Al}_2\text{Se}_{3.53}$ suggest a glass-like transition, but no intersite mixing between Co^{2+} and Al^{3+} was observed from the XPS

measurements, indicating the observed spin-freezing transition should not be induced by intersite mixing disorder. The strong magnetic frustration in $\text{Co}_{0.66}\text{Al}_2\text{Se}_{3.53}$ and $\text{Ni}_{0.61}\text{Al}_2\text{Se}_{3.55}$ should originate from the relatively small spin of $\text{Co}_{0.66}\text{Al}_2\text{Se}_{3.53}$ and $\text{Ni}_{0.61}\text{Al}_2\text{Se}_{3.55}$.

SUPPLEMENTARY MATERIAL

The supplementary material for this article can be found at <https://doi.org/10.1017/S0885715618000507>.

DISCLOSURES

The authors declare no competing financial interests.

ACKNOWLEDGEMENTS

This work was supported by the National Natural Science Foundation of China (Grant No. 51772322), Starting-up for 100 talent of Chinese Academy of Sciences and the National Key Research and Development Program of China through Contract Nos. 2016YFA0300600 and 2017YFA0304700.

Anderson, P. W. (1973). "Resonating valence bonds: a new kind of insulator?" *Mater. Res. Bull.* **8**(2), 153–160.

Anderson, P. W. (1987). "The resonating valence bond state in La_2CuO_4 and superconductivity," *Science* **235**(4793), 1196.

Balents, L. (2010). "Spin liquids in frustrated magnets," *Nature* **464**(7286), 199–208.

Chen, X., Liang, J., Xie, S., Qiao, Z., Tong, X., and Xing, X. (1992). Superconductivity and magnetic properties in $\text{Pr}_{0.2}\text{Yb}_{0.8-x}\text{La}_x\text{Ba}_2\text{Cu}_3\text{O}_{7-\delta}$. *Z. Phys. B Condens. Matter* **88**, 1–4.

Chen, X., Liang, J., Tang, W., Wang, C., and Rao, G. (1995a). Superconductivity at 55 K in $\text{La}_{0.7}\text{Sr}_{1.3}\text{Cu}(\text{O},\text{F})_{4+\delta}$ with reduced CuO_2 sheets and apical anions. *Phys. Rev. B* **52**, 16233–16236.

Chen, X., Liang, J., and Wang, C. (1995b). "Effect of high-angle diffraction data on Rietveld structure refinement" *Acta Physica Sin.* **4**(4), 259.

Chen, X., Liang, J., Wang, Y., Wu, F., and Rao, G. (1995c). Superconductivity in $\text{Y}_{0.6}\text{Pr}_{0.4}\text{Ba}_{2-x}\text{Sr}_x\text{Cu}_3\text{O}_{7-\delta}$: the role of apical oxygen in hybridization. *Phys. Rev. B* **51**, 16444–16447.

Clark, L., Nilsen, G. J., Kermarec, E., Ehlers, G., Knight, K. S., Harrison, A., Attfield, J. P., and Gaulin, B. D. (2014). "From spin glass to quantum spin liquid ground states in molybdate pyrochlores," *Phys. Rev. Lett.* **113**(11), 117201.

Collins, M. F. and Petrenko, O. A. (1997). "Review/synthese: triangular antiferromagnets," *Can. J. Phys.* **75**(9), 605–655.

Guo, J. G., Jin, S. F., Wang, G., Wang, S. C., Zhu, K. X., Zhou, T. T., He, M., and Chen, X. L. (2010). "Superconductivity in the iron selenide $\text{K}_x\text{Fe}_2\text{Se}_2$ ($0 < x < 1$)," *Phys. Rev. B* **82**(18), 180520.

Higo, T., Ishii, R., Menard, M. C., Chan, J. Y., Yamaguchi, H., Hagiwara, M., and Nakatsuji, S. (2011). "Magnetic properties of the quasi-two-dimensional antiferromagnet $\text{Ni}_{0.7}\text{Al}_2\text{S}_{3.7}$," *Phys. Rev. B* **84**(5), 054422.

Itou, T., Oyama, A., Maegawa, S., Tamura, M., and Kato, R. (2008). "Quantum spin liquid in the spin-1/2 triangular antiferromagnet $\text{EtMe}_3\text{Sb}[\text{Pd}(\text{dmit})_2]_2$," *Phys. Rev. B* **77**(10), 104413.

Jin, S. F., Huang, Q., Lin, Z. P., Li, Z. L., Wu, X. Z., Ying, T. P., Wang, G., and Chen, X. L. (2015). "Two-dimensional magnetic correlations and partial long-range order in geometrically frustrated CaOFeS with triangle lattice of Fe ions," *Phys. Rev. B* **91**(9), 094420.

Jin, S. F., Fan, X., Wu, X. Z., Sun, R. J., Wu, H., Huang, Q. Z., Shi, C. L., Xi, X. K., Li, Z. L., and Chen, X. L. (2017). "High- T_c superconducting phases in organic molecular intercalated iron selenides: synthesis and crystal structures," *Chem. Commun.* **53**(70), 9729–9732.

Krizan, J. W. and Cava, R. J. (2014). " NaCo_2F_7 : a single-crystal high-temperature pyrochlore antiferromagnet," *Phys. Rev. B* **89**(21), 214401.

Kurosaki, Y., Shimizu, Y., Miyagawa, K., Kanoda, K., and Saito, G. (2005). "Mott transition from a spin liquid to a Fermi liquid in the spin-frustrated organic conductor $\text{kappa}-(\text{ET})_2\text{Cu}_2(\text{CN})_3$," *Phys. Rev. Lett.* **95**(17), 177001.

Lai, X. F., Chen, X. L., Jin, S. F., Wang, G., Zhou, T. T., Ying, T. P., Zhang, H., Shen, S. J., and Wang, W. Y. (2013). "New layered iron sulfide $\text{NaFe}_{1.6}\text{S}_2$: synthesis and characterization," *Inorg. Chem.* **52**(22), 12860–12862.

Lai, X. F., Jin, S. F., Chen, X., Zhou, T. T., Ying, T. P., Zhang, H., and Shen, S. J. (2014). "New layered manganese selenide KMnAgSe_2 : structure and properties," *Mater. Express* **4**(4), 343–348.

Li, K. K., Huang, Q. Z., Zhang, Q. H., Xiao, Z. W., Kamiya, T., Hosono, H., Yuan, D. D., Guo, J. G., and Chen, X. L. (2018). " $\text{CsFe}_{4-\delta}\text{Se}_4$: a new compound closely related to alkali intercalated FeSe superconductors," *Inorg. Chem.* **57**(8), 4502–4509.

Li, K. K., Jin, S. F., Guo, J. G., Xu, Y. P., Su, Y., Feng, E., Liu, Y., Zhou, S. Q., Ying, T. P., Li, S. Y., Wang, Z. Q., and Chen, X. L., (submitted). "Unusual double-peak specific heat and spin freezing in a spin-2 triangular lattice antiferromagnet FeAl_2Se_4 ," *Phys. Rev. Lett.*

Lu, X. F., Wang, N. Z., Zhang, G. H., Luo, X. G., Ma, Z. M., Lei, B., Huang, F. Q., and Chen, X. H. (2014). "Superconductivity in $\text{LiFeO}_2\text{Fe}_2\text{Se}_2$ with anti-PbO-type spacer layers," *Phys. Rev. B* **89**(2), 020507.

Mandale, A. B., Badrinarayanan, S., Date, S. K., and Sinha, A. P. B. (1984). "Photoelectron-spectroscopic study of nickel, manganese and cobalt selenides," *J. Electron. Spectrosc. Relat. Phenom.* **33**(1), 61–72.

McGuire, G. E., Schweitzer, G. K., and Carlson, T. A. (1973). "Core electron binding energies in some Group IIIA, VB, and VIB compounds," *Inorg. Chem.* **12**(10), 2450–2453.

Mydosh, J. A. and Ebrary, I. (1993). *Spin Glasses: An Experimental Introduction* (Taylor & Francis, London).

Nakatsuji, S., Nambu, Y., Tonomura, H., Sakai, O., Jonas, S., Broholm, C., Tsunetsugu, H., Qiu, Y., and Maeno, Y. (2005). "Spin disorder on a triangular lattice," *Science* **309**(5741), 1697–1700.

Nakatsuji, S., Tonomura, H., Onuma, K., Nambu, Y., Sakai, O., Maeno, Y., Macaluso, R. T., and Chan, J. Y. (2007). "Spin disorder and order in quasi-2D triangular Heisenberg antiferromagnets: comparative study of FeGa_2S_4 , $\text{Fe}_2\text{Ga}_2\text{S}_5$, and NiGa_2S_4 ," *Phys. Rev. Lett.* **99**(15), 157203.

Rodríguez-Carvajal, J. (2001). "Recent developments of the program FULLPROF," *IUCr CPD-News*. **26**, 12–19.

Shimizu, Y., Miyagawa, K., Kanoda, K., Maesato, M., and Saito, G. (2003). "Spin liquid state in an organic Mott insulator with a triangular lattice," *Phys. Rev. Lett.* **91**(10), 107001.

Takada, K., Sakurai, H., Takayama-Muromachi, E., Izumi, F., Dilanian, R. A., and Sasaki, T. (2003). "Superconductivity in two-dimensional CoO_2 layers," *Nature* **422**, 53.

Tu, Q. Y., Chen, X. L., Ma, B. K., Zhao, Z. X., Xu, Y. P., Hu, B. Q., and Liang, J. K. (2001). Study on the structure and superconductivity of $\text{La}_2\text{CuO}_{4+\delta}$ chemically oxidized by NaClO at 50 °C. *Supercond. Sci. Technol.* **14**, 517.

Ying, T. P., Chen, X. L., Wang, G., Jin, S. F., Zhou, T. T., Lai, X. F., Zhang, H., and Wang, W. Y. (2012). "Observation of superconductivity at 30~46 K in $\text{A}_x\text{Fe}_2\text{Se}_2$ ($\text{A} = \text{Li, Na, Ba, Sr, Ca, Yb, and Eu}$)," *Sci. Rep.* **2**, 426.

Ying, T. P., Chen, X. L., Wang, G., Jin, S. F., Lai, X. F., Zhou, T. T., Zhang, H., Shen, S. J., and Wang, W. Y. (2013). "Superconducting phases in potassium-intercalated iron selenides," *J. Am. Chem. Soc.* **135**(8), 2951–2954.

Ying, T. P., Gu, Y. Q., Chen, X., Wang, X. B., Jin, S. F., Zhao, L. L., Zhang, W., and Chen, X. L. (2016). "Anderson localization of electrons in single crystals: $\text{Li}_x\text{Fe}_7\text{Se}_8$," *Sci. Adv.* **2**(2), e1501283.

Zha, W., Zhou, Z., Zhao, D., and Feng, S. (2016). "Positive effects of Al^{3+} partially substituted by Co^{2+} cations on the catalytic performance of $\text{Co}_{1+x}\text{Al}_{2-x}\text{O}_4$ ($x = 0-0.2$) for methane combustion," *J. Sol-Gel Sci. Technol.* **78**(1), 144–150.

Zhou, T. T., Wang, Y., Jin, S. F., Li, D. D., Lai, X. F., Ying, T. P., Zhang, H., Shen, S. J., Wang, W., and Chen, X. L. (2014). "Structures and physical properties of layered oxyselenides $\text{Ba}_2\text{MO}_2\text{Ag}_2\text{Se}_2$ ($\text{M} = \text{Co, Mn}$)," *Inorg. Chem.* **53**(8), 4154–4160.